30th International Symposium on Space Flight Dynamics (ISSFD)

Combining Differential Algebra and Subset Simulation for Efficient Long-Term Collision Risk Assessment

Andrea Zollo [(1)], Annarita Trombetta [(1)], Cristina Parigini [(2)], Roberto Armellin [(2)], Juan Félix San Juan Díaz [(3)], Ralph Kahle [(1)]

[(1)] German Space Operations Centre (GSOC), DLR, Münchener Str. 20, 82234, Weßling, Germany, email: {annarita.trombetta, andrea.zollo, ralph.kahle}@dlr.de
[(2)] Te Pūnaha Ātea - Space Institute, University of Auckland, Private Bag 92019, 1142, Auckland, New Zealand, email: {cristina.parigini, roberto.armellin}@auckland.ac.nz
[(2)] Scientific Computation & Technological Innovation Center, University of La Rioja, Madre de Dios 53, 26006, Logroño, La Rioja, Spain, email: juanfelix.sanjuan@unirioja.es

***Abstract*: This paper presents a methodology to enhance the GSOC Collision Avoidance System (CAS) for better assessing collision risk during long-term close approaches. The technique employs Differential Algebra (DA) to model the non-linear relative motion via high-order Taylor polynomial expansions, with accuracy maintained with Automatic Domain Splitting (ADS) that subdivides the initial uncertainty set. By sampling the initial relative conditions and evaluating the polynomial expansions over time, the method reduces traditional Monte-Carlo (MC) integration to a one-dimensional polynomial evaluation. Computational efficiency is further improved by integrating the Subset Simulation (SS) algorithm, an estimation technique that drastically reduces the required samples by reformulating a rare event as a sequence of more probable conditional events. The methodology's performance is evaluated, using representative synthetic benchmark scenarios from the literature as well as a real long-term encounter.**

I. INTRODUCTION

With the rapid advancement of space technology, spacecraft launches have become more frequent, leading to increased congestion in Earth's orbits. This growing density, driven largely by the accumulation of space debris, poses escalating risks to spacecraft operations. The situation is expected to worsen with the expansion of large satellite constellations, further crowding key orbital regions. As a result, operators face more frequent close-approach warnings and must carry out a rising number of Collision Avoidance Manoeuvres (CAMs) to ensure mission safety [1]. A key aspect of managing these events is the assessment of their criticality, which mainly relies on evaluating the Probability of Collision (Pc) between the objects involved.

Collision risk assessment methods are tailored to different types of conjunctions, typically classified as short-term or long-term encounters. In short-term cases, satellites follow markedly different orbits, leading to very high relative velocities and encounters lasting only a few seconds. The relative motion can be approximated as linear with a constant relative velocity vector, and associated uncertainty negligible. As a result, the combined positional uncertainty remains constant and can be described by fixed covariance matrices. This simplified scenario has been widely studied, with numerous established methods available in the literature [2, 3, 4, 5, 6, 7, 8].

Long-term encounters, on the other hand, typically occur between satellites on similar orbits, such as Geostationary (GEO) spacecrafts at close longitudes or during operations like rendezvous and formation flying. These cases involve low relative velocities and prolonged proximity, often lasting a significant fraction of an orbital period. Unlike short-term encounters, the relative motion is non-rectilinear, with the relative velocity vector changing in both magnitude and direction. As a result, the uncertainty in the relative state evolves over time rotating and deforming, leading to a time-varying covariance and complex, difficult-to-integrate collision geometries.

Collision risk assessment for long-term encounters has been less extensively studied than for short-term cases. Early approaches in the literature [9, 10, 11] discretize the collision tube into small segments, treating each as an independent short-term encounter. Other methods [12, 13] improve the geometric description of the collision volume by representing it as a swept envelope of ellipsoids, but they generally neglect velocity uncertainty. Reference [14] on the other hand, presents a more comprehensive framework that, for the first time, incorporates velocity uncertainty into the formulation. However, the method assumes a single continuous encounter geometry and does not explicitly address situations involving multiple distinct close-approach intervals within the same screening window, limiting its applicability to more complex long-term encounter scenarios. In addition, the method assumes that the uncertainty distribution remains Gaussian throughout its evolution, a constraint that can significantly restrict its use in more general scenarios. Currently, Monte Carlo (MC) based techniques [15] are among the most comprehensive approaches for long-term encounters Pc estimation, as they can account for uncertainties in both

position and velocity, handle complex encounter geometries, and avoid restrictive assumptions on the evolution of the uncertainty distribution. They also provide a natural framework for Pc computation without explicitly defining the integration volume, making them a common benchmark for validating new methods due to their high accuracy. Their main drawback, however, is the significant computational cost. To address this, recent work by the authors [16, 17] are relying on Differential Algebra (DA) [18] to significantly reduce computational time while preserving the advantages of a standard MC approach. The methodology in question models the dynamical evolution of the relative state of the objects involved in a close approach as a patched 7D continuum, where each patch is represented by a high-order Taylor expansion with respect to both time and the initial conditions at t_0. The integration accuracy of the dynamical flow is controlled by the Automatic Domain Splitting (ADS) algorithm [19], which adaptively subdivides the initial domain of the combined covariance to preserve the precision of the Taylor approximation. The initial combined covariance is then sampled to generate specific realizations of the relative state at t_0. Each patch is then evaluated accordingly to obtain a time-dependent Taylor expansion of the miss distance, which can be directly manipulated through polynomial algebra to compute the Pc, avoiding the need for conventional MC sample-by-sample propagation and collision checking.

Within the scope of this research, this paper presents a further enhancement of the methodology, marking an important step toward its operational implementation. In particular, the proposed improvement integrates the Subset Simulation (SS) technique [20, 21, 22, 23], into the problem formulation, furtherly optimising the computational speed and significantly enhancing the capabilities of the DLR German Space Operations Centre's (GSOC) Collision Avoidance System (CAS). In operational conjunction risk assessment, the Pc is typically very small, meaning that a standard MC approach requires a very large number of samples to achieve statistically reliable estimates. This makes SS particularly well suited for orbital conjunction problems, as it is specifically designed for rare-event Pc estimation while substantially reducing the required sampling effort. More specifically, the algorithm described in [17] is adapted to estimate the final Pc by decomposing the rare collision event into a sequence of intermediate conditional events of progressively increasing criticality. This guides the sampling process toward the regions of the initial relative state uncertainty that are most likely to generate collision trajectories at future times. Compared with alternative techniques, the proposed methodology avoids restrictive assumptions, such as neglecting velocity uncertainty or assuming the covariance evolution as Gaussian, while remaining robust in complex encounter scenarios involving multiple close approaches. At the same time, unlike standard MC simulations based on sample-by-sample propagation, it exploits a polynomial representation of the covariance evolution over time. This enables collision assessment through the evaluation of mono-dimensional time polynomials, significantly reducing computational cost and providing a flexible framework for integrating MC acceleration techniques such as SS.

The paper is structured as follows: Section II reviews the standard MC formulation for Pc estimation. Section III, details how DA and ADS are employed to model the dynamical evolution of initial conditions. Section IV introduces the SS algorithm and its integration, while Section V validates the approach on benchmark and real-world conjunction scenarios, in terms of accuracy and computational efficiency. Finally, Section VI summarizes the main findings.

II. PROBLEM DESCRIPTION

The statistical event F, for which a collision occurs, is introduced as follows: given the initial distribution of the state for two space resident objects at time t_0, the Hard-Body Radius (HBR) [3] and a maximum period of interest T, a collision is deemed to occur if there exists a time t, within the interval $I = [t_0, t_0 + T]$, such that the norm of the relative distance vector $\boldsymbol{d}(t)$, is less than or equal to HBR. To assess the likelihood of F occurring, and consequently characterize the Pc in a comprehensive and general manner, we introduce the relative state vector of the two objects engaged in the encounter, $\boldsymbol{x}(t)$ as

$$\boldsymbol{x}(t) = \begin{pmatrix} \boldsymbol{d}(t) \\ \boldsymbol{v_{rel}}(t) \end{pmatrix}, \tag{1}$$

in which $\boldsymbol{v_{rel}}$ is the relative velocity of the secondary object with respect to the primary. It is important to emphasize that $\boldsymbol{x}(t)$ is defined as the difference, expressed in an inertial reference frame, between the individual states of the two objects involved in a close approach denoted as $\boldsymbol{x_p}(t)$ and $\boldsymbol{x_s}(t)$, respectively. These two quantities represent six-dimensional general multivariate random variables, which may follow arbitrary distributions. However, within the scope of this study, they are assumed to be statistically independent, implying that their cross-covariance is zero. Let $\boldsymbol{x}(t_0) = \boldsymbol{x_0}$ denote the relative state vector at t_0. Given its associated PDF, $\boldsymbol{\rho_0}(\boldsymbol{x_0}, t_0)$, the Pc can be defined, without loss of generality, as:

$$\mathrm{Pc} = \mathrm{P}(F) = \mathrm{P}(\boldsymbol{x_0} \in \boldsymbol{V}) = \int_{\boldsymbol{V}} \boldsymbol{\rho_0}(\boldsymbol{x_0}, t_0)\, d\boldsymbol{x_0} \tag{2}$$

where $\boldsymbol{V} \subseteq \mathbb{R}^6$ represents the initial set for which a collision occurs at some future time t. The set $\boldsymbol{V}$ takes the name of failure region and can be interpreted as a sub-region of the multi-dimensional space $\mathbb{R}^6$ in which every realization of the random vector $\boldsymbol{x_0}$ inevitably leads to a violation of the condition $\|\boldsymbol{d}(t)\| \leq HBR$ at

a future time t; in MC methods terminology this condition is commonly referred to as the performance function. The set $\boldsymbol{V}$ is mathematically represented as:

$$\boldsymbol{V} = \{\boldsymbol{x_0} \in \mathbb{R}^6 : \exists\, t \in I : \|\boldsymbol{d}(t)\| - HBR \leq 0\} \qquad (3)$$

By definition of PDF, the 6D integral of the initial statistic over the set $\boldsymbol{V}$ yields, in fact, the probability that $\boldsymbol{x_0} \in \boldsymbol{V}$ and therefore the likelihood of the statistical event F occurring. Notably, the integrand in Eq. (2) represents the PDF of an arbitrary distribution. Hence, the methodology outlined in the following section is capable of handling the dynamical evolution of any statistical distribution, provided that its form is known a priori at t_0. Although the approach is not limited to any specific distribution, for the purposes of the present analysis, $\boldsymbol{\rho_0}(\boldsymbol{x_0}, t_0)$ is modelled as Gaussian. This choice is justified by the fact that, at least at t_0, the relative state $\boldsymbol{x_0}$ typically results from an orbit determination process, for which the Gaussian assumption is generally considered reasonable. Thus:

$$\boldsymbol{\rho_0}(\boldsymbol{x_0}, t_0) = \frac{e^{\left(-\frac{1}{2}(\boldsymbol{x_0}-\boldsymbol{\mu_0})^T \boldsymbol{P_0}^{-1}(\boldsymbol{x_0}-\boldsymbol{\mu_0})\right)}}{\sqrt{(2\pi)^6}\sqrt{\|\boldsymbol{P_0}\|}} \qquad (4)$$

where $\boldsymbol{\mu_0}$ and $\boldsymbol{P_0}$ represent respectively the mean and the covariance matrix of $\boldsymbol{x_0}$. One way of computing the integral in Eq. (2) is via a MC-based method. In fact, in such cases, the initial conditions $\boldsymbol{x_0}$ are sampled and trajectories over the time interval $[t_0, t_0 + T]$ are computed according to some dynamical model that propagates the relative state from time t_0 to T. The dynamics are usually expressed as an Ordinary Differential Equation (ODE) of the form:

$$\begin{cases} \dot{\boldsymbol{x}}(t) = f(\boldsymbol{x}(t_0), \boldsymbol{x}(t), \boldsymbol{u}(t), t) \\ \boldsymbol{x}(t_0) = \boldsymbol{x_0} \end{cases}, \qquad (5)$$

where the vector $\boldsymbol{u}(t)$ represents an eventually modelled maneuver in the relative dynamics. It is worth noting that even when the initial conditions are modelled as Gaussian, their propagation through the dynamics described in Eq. (5), which, in the context of long-term encounters, are nonlinear, generally leads to a loss of Gaussian properties in the state distribution at future times t. Finally, to compute the Pc, each sample trajectory is analysed to verify if, at some future time, a collision occurs. If one hit is recorded for a specific sample, it means that it originally belonged to the set $\boldsymbol{V}$.

III. METHODOLOGY

DA is used to model the dynamical evolution of the initial relative conditions. It provides a computational framework in which functions are represented as nth order Taylor polynomial expansions within a computer environment, rather than being treated solely as floating-point values. Accordingly, the time t can be expressed as a DA variable τ and scaled with respect to the maximum time of interest T, such that $\tau \in [-1,1]$:

$$\tau = \frac{2(t-t_0)}{T} - 1\,. \qquad (6)$$

Similarly, we introduce a vector of DA variables, $\delta\boldsymbol{x_0}$, representing the deviation of the initial relative state vector from $\boldsymbol{\mu_0}$. Each component is normalized by the maximum expected variation, $\Delta\boldsymbol{x_0}$, such that it is defined within the interval [-1,1]. This is

$$\delta\boldsymbol{x_0} = \frac{\boldsymbol{x_0}-\boldsymbol{\mu_0}}{\Delta\boldsymbol{x_0}}. \qquad (7)$$

The relative state at a given scaled instant τ, can now be computed via integration of the dynamics described in Eq. (5) and expressed in the DA framework as:

$$\boldsymbol{x} = \mathcal{T}_{\boldsymbol{x}}(\tau, \delta\boldsymbol{x_0})\,. \qquad (8)$$

$\boldsymbol{x}$ is a vector of high order polynomials that are functions of τ and the initial normalized relative statistics, $\delta\boldsymbol{x_0}$. The Taylor map $\mathcal{T}_{\boldsymbol{x}}$ establishes a relationship between the perturbed initial state vector and the corresponding state vector at a specified time within $\boldsymbol{I}$, utilizing the dynamical model defined in (5). This mapping from the initial set to the final one bears conceptual similarity to the mathematical notion of a manifold. Within the context of this research, the employed dynamical model may be arbitrarily complex and may include highly nonlinear relative motion. The only requirement is that it must be described by an analytical law that establishes a functional relationship between the state at time t and the initial conditions at t_0. Utilizing DA in this context offers several advantages. Firstly, it enables the representation of an infinite set solely through its Taylor expansion coefficients. This preserves a specific analytical structure in contrast to a mere point-wise set representation. Secondly, and perhaps most significantly, it allows the propagation of entire sets through a function using straightforward DA arithmetic operations. Unlike a standard MC simulation, where the ODE flow of Eq. (5) is integrated for each sample, in this scenario, only a single integration is required. The resulting DA expansion represents the outcome of propagating all points from the initial domain through the ODE in (5).

The challenging part of this approach arises from the nonlinear dynamics involved usually in long-term encounters. When the Taylor map needs to approximate a strongly non-linear function, the convergence of the ODE expansion across the domain becomes inaccurate. Consequently, the DA map, which is a local representation of the function, poorly represents the actual evolution over the whole domain, even though the description is accurate in the vicinity of the centre of the expansion. To address this issue, we employ the technique proposed in [19]. The ADS algorithm detects when the polynomial expansion of the ODE flow over the initial conditions no longer provides a sufficiently

accurate representation of the dynamics. When this occurs, the original expansion domain is split along one of the expansion variables into two subdomains. This procedure is repeated iteratively until the desired accuracy is maintained, resulting in the initial 7D domain, defined by the variables $\boldsymbol{\tau}$ and $\delta\boldsymbol{x_0}$, being partitioned into multiple subdomains. As a result, the dynamical evolution of the initial condition assumes the shape of a patched 7D continuum, mathematically defined as a manifold object. A Taylor expansion in $\boldsymbol{\tau}$ and $\delta\boldsymbol{x_0}$, locally approximating the dynamical flow, corresponds to each patch at a given time. Once a single integration has been performed and the evolution of the initial condition is approximated by patched polynomials, our methodology proceeds to calculate the function d^2 within the DA framework:

$$d^2 = \mathcal{T}_{d^2}(\tau, \delta\boldsymbol{x_0}) \tag{9}$$

Here, d^2 is a high order polynomial representation of the relative distance squared expressed as function of time and the initial state. It is again piece-wise defined, and its definition interval depends on the ADS accuracy control algorithm. At this stage, the performance function can be formulated within the DA framework as:

$$g(\tau, \delta\boldsymbol{x_0}) = d^2 - HBR^2 \tag{10}$$

The expression in Eq. (10) represents the DA formulation of the condition introduced in Eq. (3) and is fully equivalent to it, providing the criterion for identifying the failure region $\boldsymbol{V}$. The methodology then proceeds by sampling $\boldsymbol{x_0}$. Each realization $\boldsymbol{X_{0k}}$ of the random vector is linked to its respective initial patch and evaluated only in space and velocity. This evaluation reduces the dimensions of the d^2 polynomials, resulting in a set of one-dimensional Taylor expansions depending solely on time:

$$g_k(\tau) = d^2(\tau, \delta\boldsymbol{x_0} = \boldsymbol{X_{0k}}) - HBR^2 \tag{11}$$

This expansion holds significant importance as it enables collision assessment for each sample, replacing the classical MC propagation with the treatment of a high order polynomial approximation of the sample trajectory.

IV. Subset Simulation Algorithm

This section focuses on the sampling process introduced in Eq. (11) and explains how the DA expansions are finally used to compute the final Pc. Specifically, it introduces the underlaying principles of the SS algorithm and how it has been integrated into the DA formulation with the aim of reducing the total number of samples required and drastically reducing the final computational time. Readers interested in a more detailed description of the SS algorithm are referred to [21, 22]. The core idea of SS is to reformulate the estimation of a small rare-event probability $P(F)$ as a sequence of more frequent conditional probability events. To achieve this, the event F, described in section II, can be seen as the union of a nested sequence of m intermediate collision events F_i, each one with corresponding failure region V_i:

$$F_1 \supset F_2 \supset F_i \supset \cdots \supset F_m = F \tag{12}$$

This simple intuition is crucial, as it enables the use of the probability chain rule, allowing $P(F)$ to be rewritten as the product of conditional probabilities across consecutive subsets:

$$P(F) = P(F_1)\prod_{i=1}^{m-1} P(F_{i+1} \mid F_i) \tag{13}$$

Where $P(F_{i+1} \mid F_i)$ represents the probability of F_{i+1} conditional to F_i. In Eq. (13), each conditional probability is deliberately selected to be much larger than the final $P(F)$. Intuitively, these intermediate levels can be understood as a sequence of statistical events in which the collision threshold in Eq. (10) is artificially enlarged, making collisions progressively more likely than in the original problem:

$$c_1 > c_2 > c_i > \cdots > c_m = HBR^2 \tag{14}$$

The method begins with a standard MC sampling of the initial uncertainty, generating a starting set of N_T samples at the so called first Conditional Level (CL0), denoted as $\boldsymbol{X_{0k}^{CL0}}$ with $k = 1, \dots, N_T$. The DA representation of the performance function in Eq. (10) is evaluated as described in Eq. (11), yielding for each sample a time-dependent polynomial representation of its trajectory, piecewise defined according to the domain bounds of each polynomial patch. The minimum value of each $g_k(\tau)$, and therefore of each patched trajectory, is computed. The initial set of N_T samples is then ranked in ascending order based on the corresponding minimum value of the performance function.

A constant intermediate probability of failure, P_0, is then selected and maintained across all subsequent CLs. P_0 identifies the samples belonging to the failure region by selecting those with performance function values smaller than or equal to the $P_0 N_T$th element of the sorted sample set. Equivalently, this defines an intermediate threshold, c_1, selecting the trajectories that satisfy the corresponding collision condition at CL0. Starting from these selected samples, new conditional samples $\boldsymbol{X_{0k}^{CL1}}$ are generated using a Markov Chain Monte Carlo (MCMC) approach, ensuring that the new candidates remain within the identified subset. In this work, the adaptive-sigma Metropolis-Hastings approach proposed by [22] is employed. The same procedure is then repeated to determine successive intermediate failure regions and generate additional conditional samples, progressively driving the simulation toward the target failure domain until the actual failure region is reached. The final algorithm can be summarised with the

following steps:

1. Initialise a counter $i = 0$ that iterates over m CLs.
2. Generate N_T samples $\boldsymbol{X_{0k}^{CL0}}$ with $k = 1, \dots, N_T$ for CL0 by classic MC sampling.
3. Evaluate the DA Taylor polynomial map in each $\boldsymbol{X_{0k}^{CLi}}$ as in Eq. (11) and compute the minimum of $g_k(\tau)$.
4. Sort the N_T samples in ascending order, according to the minimum value of their corresponding $g_k(\tau)$.
5. Choose the intermediate threshold value c_{i+1} as the $P_0 N_T$th value of the sorted list. The next event is defined as $F_{i+1} = \{d^2 < c_{i+1}\}$. By definition, the associated conditional probability is: $P(F_{i+1} \mid F_i) = P(d^2 < c_{i+1} \mid d^2 < c_i) = P_0$.
6. If $c_{i+1} \leq HBR^2$ go to step 9, otherwise identify the $P_0 N_T$ samples as the ones belonging to CL $i+1$.
7. Using MCMC, generate $(1 - P_0)N_T$ additional conditional samples starting from the previously selected seeds belonging to F_{i+1}.
8. Set $i = i + 1$ and return to step 3.
9. Stop the algorithm and compute the final probability of collision as:

$$P_c = P_0^{m-1} \frac{N_F}{N_T}, \tag{15}$$

Where m denotes the total number of CLs generated during the iterative procedure, N_T is the number of samples at each CL and N_F represents the number of colliding samples at the last conditional level m.

A visual interpretation of how the algorithm works is provided in Fig. 1, based on a test case that is described in details in the following section. Fig. 1–(a) illustrates the samples generated through a crude MC simulation, with failure regions framed in an orange rectangle and the corresponding hitting samples in blue. Fig. 1–(b) shows the samples generated by the SS algorithm for the same initial conditions. Samples from different CLs are shown in different colours, highlighting how the algorithm progressively drives the sampling process toward the failure region and the collision-causing subsets of the uncertainty domain.

The SS offers the advantage of reducing the number of required samples to $N = N_T + (m-1)(1 - P_0)N_T$ and to thus lower the computational time compared to a classical MC approach. Despite this, the main bottleneck remains the evaluation of the performance function. This step is computationally demanding, since it would require sample-by-sample orbital propagation over the desired time span. The main advantage of combining SS with DA (DASS) is that the stochastic sampling is performed on a precomputed representation of the dynamics in Eq. (5), thereby avoiding repeated numerical integration during the Pc estimation. This last is then obtained by evaluating the patched continuum in the state space and computing the minimum of a series of high-order polynomial in time, all without imposing assumptions on the evolution of position and velocity uncertainties.

V. TESTING

The performance of the methodology was first assessed using test cases #2 and #5 from [15], two well-established benchmark scenarios commonly adopted in the literature for long-term orbital conjunction analysis conjunctions. Test case #2 is particularly relevant because it exhibits two clearly separated failure regions, as shown in Fig. 1. Test case #5, on the other hand, is characterized by a moderately large number of collision samples, making it well suited for evaluating and tuning the algorithm parameters. The efficiency of the DASS in fact relies on the proper selection of the intermediate probability of failure P_0, the number of samples per conditional level N_T and the shape of the proposal PDF for the generation of the Markov chain.

The results of the analysis are summarised in Tab. 1, where the performance of the DASS methodology is compared with a standard MC approach under two different relative dynamics models: the Clohessy-Wiltshire (CW) [24] and the Yamanaka-Ankersen (YA) [25] formulations. In all simulations, the maximum initial variation $\Delta \boldsymbol{x_0}$ for the DA is assumed to be 5σ, while the intermediate failure probability P_0 is set to 0.2, consistent with the recommended range $P_0 \in [0.1; 0.3]$ reported in [23], and N_T is fixed at 30,000. The proposal PDF adopted in the MCMC sampling is a univariate Gaussian distribution, with its variance adaptively selected according to [22]. A first notable result is the computational efficiency of the methodology, which achieves speed-ups of one to three orders of magnitude compared with crude MC, while keeping the estimation error relative to reference below 0.58%. The standard deviation of the final estimated Pc, on the other hand, is consistently about one order of magnitude higher than that obtained with standard MC. This behaviour is generally expected and represents the trade-off for achieving a substantial reduction in the total number of samples. In fact, at each conditional level, the estimate is based on a smaller number of samples than in crude MC, which inherently increases sampling variability. Moreover, these samples are generated through Markov Chains and are therefore statistically correlated, reducing the effective sample size compared with an equivalent set of independent samples. Since the variance of a MC estimator scales inversely with the effective sample size, both effects contribute to an increase in the variance of the conditional estimates. This uncertainty then propagates through the successive conditional levels and accumulates in the computation of the final Pc estimate through Eq. (13). Fig. 2-(a) and (b) illustrate the impact of N_T on the variability of the

final estimates. Gaussian fits over 50 simulations with different seeds for each test case show that increasing N_T reduces the standard deviation, bringing it closer to that of a crude MC, with a corresponding increase in computational cost. These considerations regarding the results variability are not particularly limiting, as this effect becomes less significant when the target Pc is very small. As the event becomes rarer, crude MC is increasingly affected by few hit statistics, whereas SS preserves statistically informative sampling through intermediate conditional levels, resulting in a more stable estimate. This is ultimately the relevant regime, where Pcs in conjunction risk assessment operations are typically on the order of 1e-4 or lower.

The methodology is also evaluated on a real long-term conjunction scenario, whose details are reported in [17]. This case is particularly relevant as it demonstrates both the capability of the methodology to handle multiple TCAs within the screening interval and its applicability in an operational setting. Fig. 3-(a) shows the evolution of the relative distance of the hitting samples over a 2-day period. The sample trajectories exhibit different minima and impact times, and are color-coded according to regions of the initial combined covariance

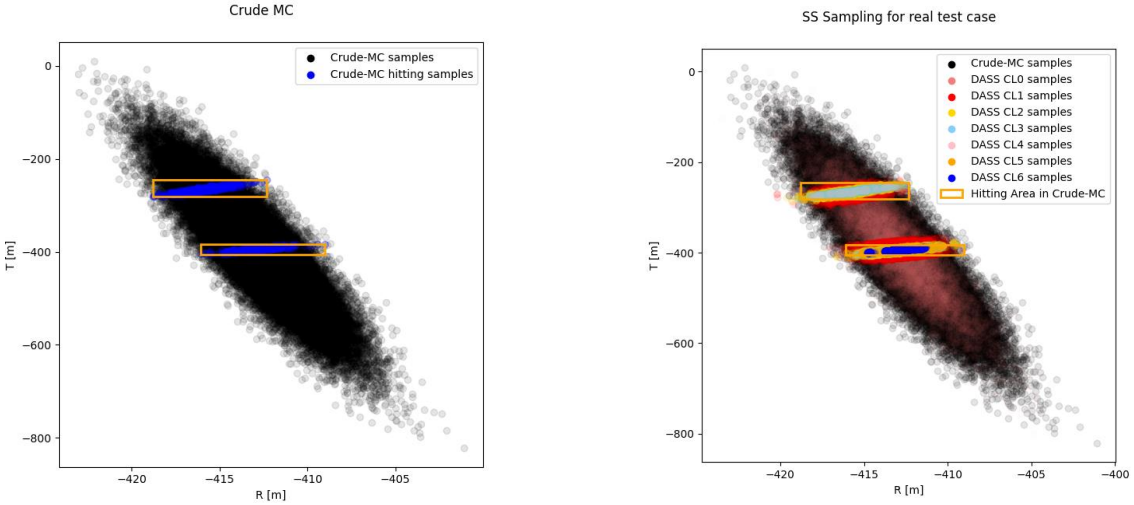

(a) **(b)**

Fig. 1: Sampled initial combined covariance of Case #02 from [15] on the R-T plane of the primary: (a) samples generated by crude MC Simulation and (b) by SS algorithm.

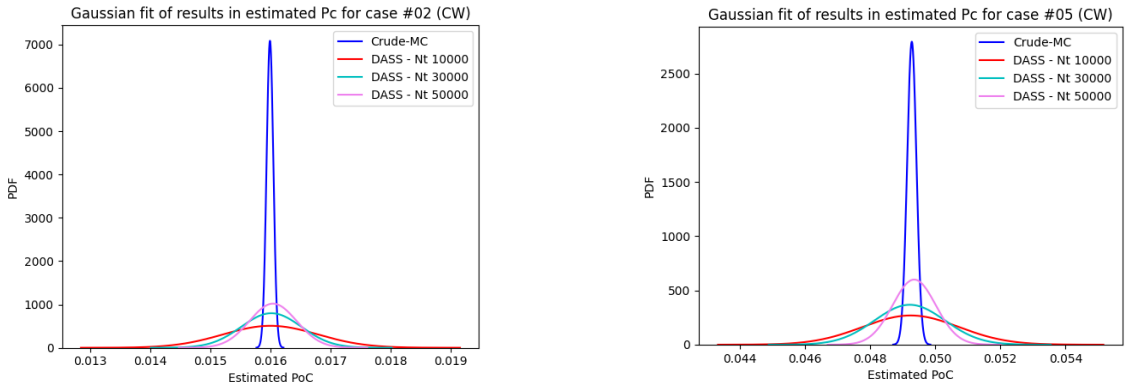

(a) **(b)**

Fig. 2: Effect of the number of samples per conditional level N_T on the variability of the final Pc estimate for test cases #2 and #5.

Test-Case	Dynamics	Method	Tot. n° Samples	Mean Pc	% Err.	Estimation σ	Cmp. Time [s]
#2	CW	MC	6.520e+06	0.015992	0.00	0.000057	3.9378e+03
		DASS	7.800e+04	0.016015	0.14	0.000506	3.0883e+01
	YA	MC	6.520e+06	0.015625	0.00	0.000048	9.4998e+04
		DASS	7.800e+04	0.015716	0.58	0.000445	4.0222e+01
#5	CW	MC	2.300e+06	0.049278	0.00	0.000144	1.6295e+03
		DASS	5.400e+04	0.049215	-0.13	0.001094	2.1419e+02
	YA	MC	2.300e+06	0.049344	0.00	0.000143	3.5586e+04
		DASS	5.400e+04	0.049587	0.49	0.000934	2.1810e+02

Table. 1: Performance comparison of DASS against standard MC for scenarios #2 and #5 from [15], using different relative dynamical models.

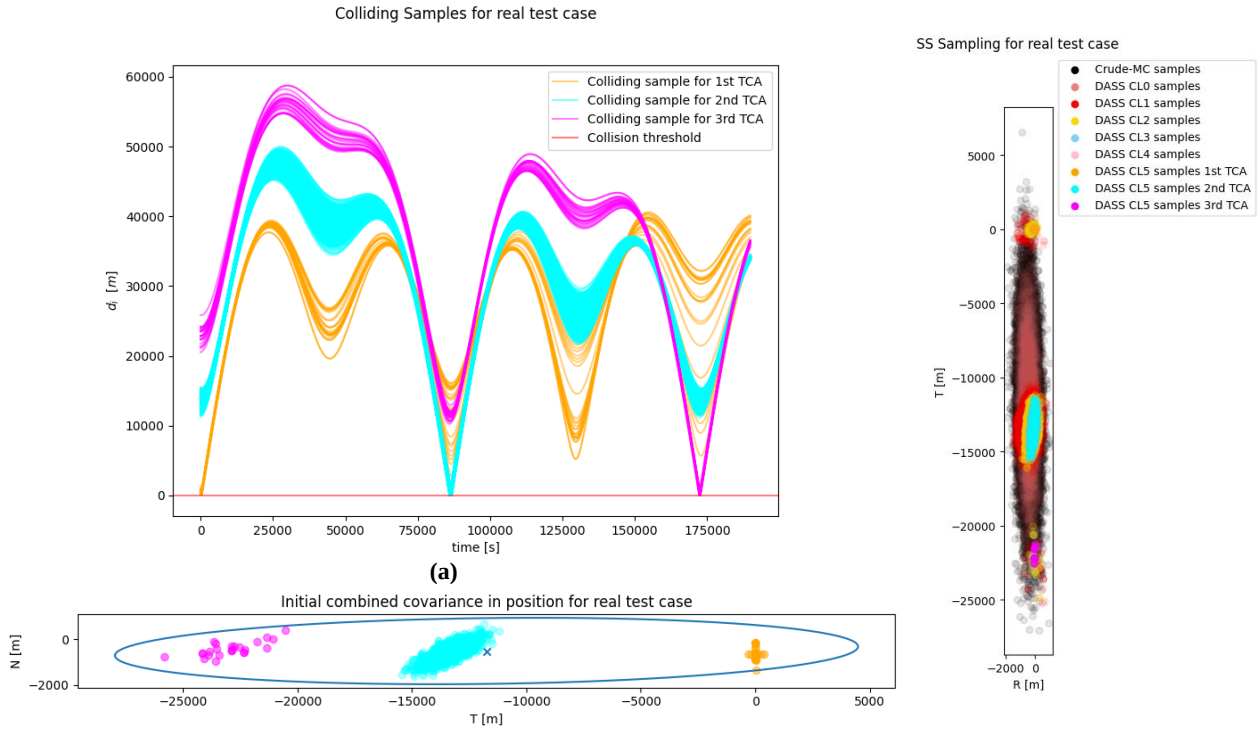

Fig. 3: Real test case scenario showing (a) the evolution of the colliding samples and (b) the corresponding impact regions within the initial combined covariance, which are accurately captured by the SS sampling process in (c).

shown in Fig. 3-(b). In particular, moving from right to left, the orange samples result in impacts a few hundred seconds after the start of the simulation, while the cyan and magenta regions correspond to the second and third TCAs, respectively. As reported in [17], the orange and magenta samples contribute with a comparable increase in Pc, on the order of 10^{-7} over time, whereas the dense cyan region yields a contribution of approximately 10^{-4}. Fig. 3-(c) shows the samples generated by the DASS algorithm, which achieve a notable convergence after five CLs toward the same failure regions identified in Fig. 3-(b). The proposed methodology is compared with a DA based MC simulation (DAMC); approach developed in [17]. Using 50,000 samples per conditional level, the SS algorithm requires a total of $2.5 \cdot 10^5$ samples, compared with $2.5 \cdot 10^9$ MC samples needed to achieve statistical significance with 5% accuracy and 95% confidence. The estimated final Pc is $1.46 \cdot 10^4$, with a relative error of 0.13% with respect to the reference method. In terms of computational time, the advantage is significant, with DAMC requiring $3.65 \cdot 10^5$ s versus $7.75 \cdot 10^2$ s for DASS. Moreover, the standard deviation of the estimate is substantially reduced compared to test cases #2 and #5, reaching $9 \cdot 10^{-6}$, consistent with the increased rarity of the event by approximately two orders of magnitude.

VI. Conclusions

Within the context of this work, we presented an improvement and a further step towards the operational implementation of an established methodology proposed by the authors for computing the Pc between two space objects, particularly suited for long-term encounters characterized by relative velocities on the order of meters per second. The proposed approach combines the computational efficiency of the SS algorithm with a DA representation of the evolution of the initial conditions in a non-linear dynamical scenario. Specifically, DA is used to model the non-linear time evolution of the multivariate initial relative state vector as a patched 7D continuum, where each patch is represented by a high-order Taylor expansion in both time and the initial conditions at t_0. The integration accuracy of the dynamical flow is controlled by the ADS algorithm, which adaptively splits the initial domain of the combined covariance to ensure precision of the Taylor approximation. The initial PDF is then sampled through the SS process, which reformulates the final Pc estimation as a sequence of higher conditional probability estimations. At each CL, the polynomial patches are evaluated over a set of samples generated through Markov Chains, each corresponding to a specific realisation of the initial state-vector, to accurately determine its time evolution. The minimum of each resulting time-dependent polynomial is then used to identify the samples belonging to the failure region at that CL. The process is repeated until convergence to the actual failure region is achieved,

with a final number of samples significantly lower than that required by a conventional MC approach. The proposed methodology retains all the advantages of a MC simulation while offering a substantial improvement in computational speed. In principle, it can be applied to any form of initial uncertainty, provided that the initial PDF is known a priori, without requiring the restrictive assumption of Gaussianity at t_0 or throughout the evolution of the initial conditions. Moreover, the approach can incorporate uncertainties in velocity and naturally accounts for multiple TCAs occurring within the screening interval. Additionally, the technique is applicable to any form of relative or absolute dynamics, provided that an analytical formulation of the dynamics is available.

The technique has been validated and tuned against benchmark test cases from the literature, and its applicability has been further demonstrated on a real operational scenario. In all cases, the estimated Pc shows excellent agreement with the corresponding MC and DAMC simulations used for validation, while achieving a total computational time that is consistently one to three orders of magnitude lower.

VII. REFERENCES

1. ESOC (European Space Operations Centre), "*ESA's annual space environment report*", ESA Space Debris Office (2025).
2. Foster, J. A., Estes, H. S. "*Parametric analysis of orbital debris collision probability and maneuver rate for space vehicles*." Technical Report. NASA JSC, 1992.
3. Patera, R. P. "*General method for calculating satellite collision probability*." Journal of Guidance, Control, and Dynamics, 2001, 24(4): 716–722.
4. Patera, R. P. "*Calculating collision probability for arbitrary space vehicle shapes via numerical quadrature*." Journal of Guidance, Control, and Dynamics, 2005, 28(6): 1326–1328.
5. Alfriend, K. T., Akella, M. R., Frisbee, J., Foster, J. L., Deok-Jin, L., Wilkins, M. "*Probability of collision error analysis*." Space Debris, 1999, 1(1): 21–35.
6. Alfano, S. "*A numerical implementation of spherical object collision probability*." The Journal of the Astronautical Sciences, 2005, 53(1): 103–109.
7. Chan, K.," *Collision probability analyses for earth orbiting satellites*". Adv. Astronaut. Sci. 96, 1033–1048, 1997
8. Serra, R., Arzelier, D., Joldes, M., Lasserre, J. B., Rondepierre, A., Salvy, B. "*Fast and accurate computation of orbital collision probability for short-term encounters*." Journal of Guidance, Control, and Dynamics, 2016, 39(5): 1009–1021
9. Patera, R. P. "*Satellite collision probability for nonlinear relative motion*." Journal of Guidance, Control, and Dynamics, 2003, 26(5): 728–733.
10. Patera, R. P. "*Collision probability for larger bodies having nonlinear relative motion*." Journal of Guidance, Control, and Dynamics, 2006, 29(6):
11. Alfano, S. "*Addressing nonlinear relative motion for spacecraft collision probability*." In: Proceedings of the AIAA/AAS Astrodynamics Specialist Conference and Exhibit, 2006: 6760
12. F.K. Chan. "*Hovering collision probability*." In AAS/AIAA Space Flight Mechanics Meeting, number AAS 15-234, Williamsburg, VA, USA, January 2015.
13. K. Chan. "*Spacecraft collision probability for long-term encounters*." Number AAS 03-549, Big Sky, Montana, USA, 2003.
14. V.T. Coppola. "*Including Velocity Uncertainty in the Probability of Collision between Space Objects*." Advances in the Astronautical Sciences, 143, 2012.
15. Alfano S., "*Satellite conjunction Monte Carlo analysis*." Advances in the Astronautical Sciences, 134:2007–2024, 2009.
16. A. Zollo, C. Parigini, R. Armellin, J. F. San Juan Díaz, S. Aida, R. Kahle, "*Long-term collision probability computation through high order polynomials evaluation*", 29th International Symposium on Space Flight Dynamics (ISSFD), Darmstadt, Germany, 22-26th April 2024
17. A. Zollo, C. Parigini, R. Armellin, J. F. San Juan Díaz, A. Trombetta, R. Kahle, "*A polynomial-based Monte Carlo approach for estimating long-term collision probabilities*", Acta Astronautica, Volume 242, 2026, Pages 178-192,
18. Armellin, R., Di Lizia, P., Bernelli Zazzera, F., Berz, M. "*Asteroid close encounters characterization using differential algebra: the case of Apophis*." Celest. Mech. Dyn. Astron. 107, 451–470 (2010)
19. A. Wittig, P. Di Lizia, R. Armellin, K. Makino, F. Bernelli-Zazzera, and M. Berz, "*Propagation of large uncertainty sets in orbital dynamics by automatic domain splitting*", Celestial Mechanics and Dynamical Astronomy, Vol. 122, No. 3, 2015, pp. 239–261.
20. M. Losacco, M. Romano, P. Di Lizia, C. Colombo, R. Armellin, A. Morselli, J. M. Sanchez Pérez, "*Advanced Monte Carlo sampling techniques for orbital conjunctions analysis and Near Earth Objects impact probability computation.".* 1st NEO and Debris conference, Darmstadt, Germany, 2019.
21. Au, S.-K., Beck, J.L., 2001. "*Estimation of small failure probabilities in high dimensions by subset simulation*." Probab. Eng. Mech. 16 (4), 263–277.
22. I. Papaioannou, W. Betz, K. Zwirglmaier, D. Straub, "*MCMC algorithms for Subset Simulation*", Probabilistic Engineering Mechanics, Volume 41, 2015, Pages 89-103
23. K.M. Zuev, J. L. Beck, S. -K. Au, L. S. Katafygiotis, "*Bayesian post-processor and other enhancements of subset simulation for estimating failure probabilities in high dimensions*." Comput. Struct. 92, 2012.
24. W. H, Clohessy, R. S.; Wiltshire, "*Terminal Guidance System for Satellite Rendezvous".* Journal of the Aerospace Sciences. (1960), 27 (9): 653–658.
25. K. Yamanaka, and F. Ankersen," New *State Transition Matrix for Relative Motion on an Arbitrary Elliptical Orbit*", Journal of Guidance, Control, and Dynamics, Volume 25, pp. 60-66, 2002